Topology optimization of supporting structure for seismic response reduction of an arch

Miyazu, Yuji; Ohsaki, Makoto; Tsuda, Seita

Submitted to Science China Technological Sciences

Topology optimization of supporting structure for seismic response reduction of an arch

Yuji MIYAZU[1], Makoto OHSAKI[2], Seita TSUDA[3]
[1]*Hiroshima University, Higashi-Hiroshima 739-8527, Japan;*
[2]*Kyoto University, Kyoto 615-8540, Japan;*
[3]*Okayama Prefectural University, Soja 719-1197, Japan*

Abstract

A flexible supporting structure that reduces seismic response of an arch is proposed. Topology and cross-sectional areas of the supporting structure modeled as a truss structure are optimized through two steps of static and dynamic optimization problems. In the first step, a flexible supporting structure that has diagonal displacement at the top under horizontal load is obtained by solving static optimization problems. Then, in the second step, the cross-sectional area of the flexible member is optimized to minimize the seismic response acceleration of the arch evaluated by the complete quadratic combination (CQC) method. Time-history seismic response analysis is carried out to show that the response in the normal direction of the roof successfully decreases due to flexibility of the supporting structure; in addition, installing passive energy dissipation devices into the flexible supporting structure is very effective in reducing the tangential response of the arch.

Keywords: topology optimization, arch, supporting structure, truss, nonlinear programming problem, CQC method

1 Introduction

The approaches to seismic response reduction of structures in the field of civil engineering are classified into stiff seismic design, passive control [1], and base isolation [2]. It is rather easy to reduce the seismic response of a building frame using one of the three approaches, because the lowest mode usually dominates in the response to horizontal seismic excitation. However, seismic response reduction of long-span structures such as shells, arches, latticed domes, and bridges are difficult, because several modes should be considered in the process of response evaluation. Ohsaki et al. [3] used the complete quadratic combination (CQC) method to incorporate the interaction of higher modes in seismic response evaluation based on the response spectrum approach. Passive control devices including tuned mass damper (TMD) and viscous dampers can be effectively used [4–6]. Base isolation can also be utilized for reduction of the seismic input energy by increasing the natural period [7]. Ohsaki and Kinoshita [8] demonstrated that the vertical responses of an arch under vertical excitation could be reduced by installing flexible supports modeled as compliant bar-joint structure.

Optimization techniques have been widely applied to seismic design of structures in civil and

architectural engineering [9–11]. Ohsaki et al. [12] presented a method for optimizing a structure with a flexible base exhibiting reverse rocking mechanism. However, in the existing researches of optimization of long-span structures, the structures are usually supported directly on the ground, or only the upper structures are optimized, although it is important to optimize the supporting structure to utilize the flexibility of support for response reduction of the upper structure. It is also important to note that acceleration responses should be reduced for long-span roof structures in the regions of high seismic risk, because the damage of non-structural components such as ceiling and hanging equipment is strongly related to response acceleration.

In this paper, the supporting structure of an arch is modeled as a pin-jointed truss structure, and its topology and the cross-sectional areas are optimized. Truss topology optimization is a well-established field of research in structural optimization [13–15]. The ground structure approach is usually used to remove the unnecessary members from a highly connected ground structure. Hajirasouliha et al. [16] optimized simple trusses considering seismic excitations. However, most of the researches on truss topology optimization are concerned with static problems.

In this paper, a two-stage method is presented for optimization of flexible supports of an arch for seismic response reduction. The supporting structure is modeled as a pin-jointed truss, and its topology is optimized using a nonlinear programming approach. The static optimization in the first step is further divided into maximization of the vertical/horizontal displacement ratio under a lateral load and minimization of total structural volume to generate a truss with few members. The stiffness of a flexible member in the support is adjusted in the second step to reduce the normal acceleration of an arch supported by the flexible truss. It is also shown that installation of a viscous damper leads to reduction of acceleration response of the arch in tangential direction.

2 Overview of flexible supporting structure

We first illustrate the feature of a flexible structure, proposed in this study, for supporting an arch, which is supposed to be a part of a cylindrical roof. In the conventional arch supported by a stiff structure, the response in the normal direction is excited even when the arch is subjected only to horizontal seismic ground motion as illustrated in Figure 1. Since the normal directional response of a roof is one of the main factors that cause buckling of roof members, damage of the attachments of a ceiling, and a fall of the ceiling and hanging equipment [17], it is important to reduce the normal directional response of the roof structure.

We design a supporting structure such that the top node moves in a diagonal direction by utilizing its flexibility, as shown in thick arrows in Figure 2, when the top node is subjected to a lateral load. We call this structure *flexible supporting structure*. It is expected that the flexible supporting structure allows the roof structure to move mainly in the tangential direction as illustrated in Figure 2 and reduces the normal directional response. At the same time, it is supposed that the tangential response would increase due to

flexibility of the support; therefore, we propose installation of passive energy dissipation devices into the supporting structure to reduce the tangential response as well.

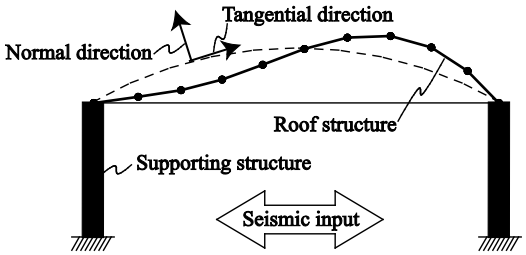

Figure 1 An arch with a conventional stiff supporting structure; solid line: deformed shape, dashed line: initial shape

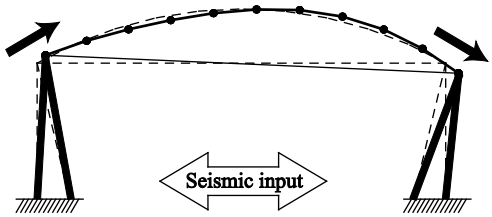

Figure 2 An arch with a flexible supporting structure; solid line: deformed shape, dashed line: initial shape

3 Static topology optimization of flexible supporting structure

The flexible supporting structure is composed of pin-jointed truss members as illustrated in Figure 3(a). The conventional ground structure approach is used for topology optimization. A supporting structure that has diagonal displacement under lateral load is generated through optimization for maximizing the ratio of vertical displacement to horizontal displacement of the top node.

The width and the height of the supporting structure are 2 m and 6 m, respectively. The ground structure is composed of 10 nodes including supports and 29 truss members. The members are not connected at their intersections without nodes. Node 3 is a pin support, and nodes 1 and 2 are roller supports. The mass of 4000 kg is attached at node 10 to represent the mass of an arch, and the weight of the truss members is ignored.

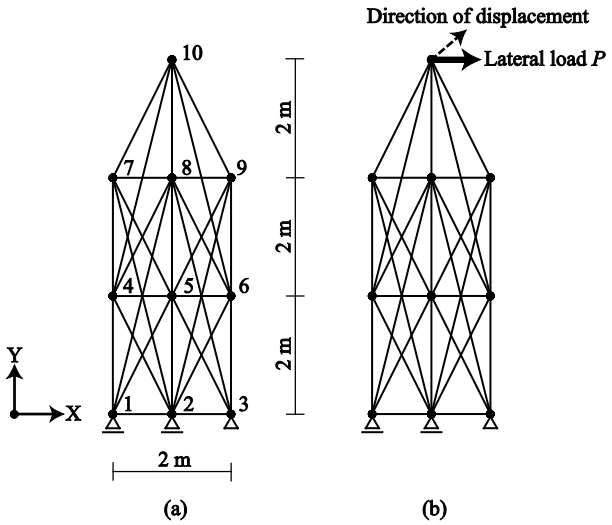

Figure 3 Ground structure for static topology optimization

We use assumption of small deformation. Therefore, in a conventional supporting structure that is symmetric with respect to the vertical center axis, its top node does not move in vertical direction under a lateral road. Here, we design a structure so that the top node moves in diagonal direction under a lateral load as illustrated in Figure 3(b). For this purpose, asymmetric properties of topology and cross-sectional areas are allowed in the formulation of optimization problem.

It may be natural to minimize the structural volume under equality constraint on the direction of top node displacement; however, optimization may terminate if no feasible solution is found. Accordingly, the objective function to be maximized is formulated as

$$R = \frac{d_{hv}}{d_{hh}}, \tag{1}$$

where d_{hv} and d_{hh} are the displacements in the vertical (Y) and horizontal (X) directions, respectively, of node 10 under a lateral load P = 7.84 kN, which corresponds to 20 % of weight of the mass at node 10.

Let d_{gh} and d_{gv} denote the X- and Y-directional displacements, respectively, under self-weight of 39.20 kN. The lower bounds d_{gh}^L = −0.012 m and d_{gv}^L = −0.006 m are given to ensure enough vertical stiffness, and the upper bound d_{hh}^U = 0.06 m is given to avoid too small stiffness against lateral load. The cross-sectional areas A_i of all m (= 29) truss members are considered as design variables, which are denoted by a vector $\mathbf{A}$ = (A_1, …, A_m). The lower bound A_i^L and the upper bound A_i^U for A_i are 1.0×10^{-6} m^2 and 2.0×10^{-3} m^2, respectively. The optimization problem called *Problem 1* is formulated as follows:

$$\begin{aligned} \text{Problem 1:}\quad & \text{Maximize} && R(\mathbf{A}) \\ & \text{subject to} && d_{gh}(\mathbf{A}) \geq d_{gh}^L, \\ & && d_{gv}(\mathbf{A}) \geq d_{gv}^L, \\ & && d_{hh}(\mathbf{A}) \leq d_{hh}^U, \\ & && A_i^L \leq A_i \leq A_i^U \qquad (i = 1, \ldots, m). \end{aligned} \tag{2}$$

The optimal solution obtained by solving Problem 1 might have unnecessary members; hence, we next minimize the total structural volume under displacement constraint. It is well-known especially in continuum topology optimization that a gray solution with many elements with intermediate value of design variables is obtained, if the total structural volume is simply minimized [18]. In the standard solid isotropic material with penalization (SIMP) approach [18], the stiffness of an element with an intermediate thickness is artificially underestimated. This approach is also applicable to frame structures [19]. An alternative approach is to overestimate the cross-sectional area for computing the structural volume, while using linear relation for stiffness computation. Bruns [20] proposed an approach using a hyperbolic function. Grudes and Taylor [21] proposed a generalized cost function. Rietz [22] used an inverse power-law for computing the structural volume. We apply this approach to truss topology optimization to reduce the number of members in the optimal solution. In this way, the design variables

exactly correspond to the stiffness of members, and the constraints are rigorously satisfied by the optimal solution if sufficiently good convergence is achieved.

Let $\tilde{\mathbf{A}} = (\tilde{A}_1, \ldots, \tilde{A}_m)$ denote the modified cross-sectional area to calculate the total volume. We use a simple inverse power-law with $p = 0.5$ as

$$\tilde{A}_i = A_i^L + \left(A_i^U - A_i^L\right) \times \left(\frac{A_i - A_i^L}{A_i^U - A_i^L} \right)^p . \tag{3}$$

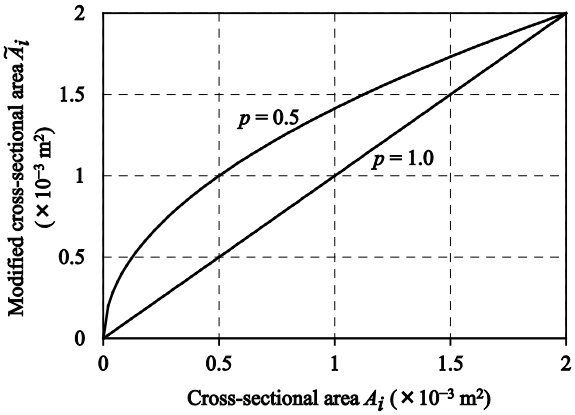

Figure 4 Relation between cross-sectional area A_i and modified cross-sectional area $\tilde{A}_i$

Figure 4 shows the relation between the cross-sectional area A_i and the modified cross-sectional area $\tilde{A}_i$ illustrated using Eq. (3) with $p = 0.5$ and 1.0, respectively. As is obvious from Figure 4, Eq. (3) with $p = 1.0$ means linear relation. It is seen that the modified cross-sectional area with $p = 0.5$ is more overestimated than that with $p = 1.0$ as the cross-sectional area A_i becomes small; therefore, it is expected that using Eq. (3) with $p = 0.5$ is effective to lead the small cross-sectional areas to their lower bound A_i^L.

Let R_{opt} denote the optimal value of $R(\mathbf{A})$ of Problem 1. It is desirable to have $R(\mathbf{A})$ that is not less than R_{opt} to retain diagonal displacement at node 10; however, R_{opt} is multiplied by a coefficient $C = 0.95$ to obtain the lower bound to have sufficiently large feasible region. The following problem called *Problem 2* is solved to minimize the total volume $V(\tilde{\mathbf{A}}(\mathbf{A}))$ of truss members and to reduce the number of members that have intermediate values of the cross-sectional areas between A_i^L and A_i^U:

$$\begin{aligned} \text{Problem 2:} \quad & \text{Minimize} \quad V\left(\tilde{\mathbf{A}}(\mathbf{A})\right) \\ & \text{subject to} \quad d_{gh}(\mathbf{A}) \geq d_{gh}^L , \\ & \qquad\qquad\; d_{gv}(\mathbf{A}) \geq d_{gv}^L , \\ & \qquad\qquad\; d_{hh}(\mathbf{A}) \leq d_{hh}^U , \\ & \qquad\qquad\; R(\mathbf{A}) \geq C R_{opt} , \\ & \qquad\qquad\; A_i^L \leq A_i \leq A_i^U \qquad (i = 1, \ldots, m) . \end{aligned} \tag{4}$$

Optimization problems 1 and 2 are solved using the optimization library SNOPT Ver. 7 [23], which uses sequential quadratic programming. A finite difference approach is used to calculate the sensitivity coefficients. The frame analysis software OpenSees [24] is used for structural analysis. Note that geometrical nonlinearity is not considered in the structural analysis.

Problem 1 is solved ten times from randomly generated ten different initial solutions. Figure 5(a) shows the best optimal solution with $R(\mathbf{A})$ = 0.517. The width of each member is proportional to its cross-sectional area A_i, and the members indicated by dashed lines have the lower-bound cross-sectional areas. The cross-sectional areas of 16 members are equal to their lower bounds; hence, those members have been removed. The cross-sectional areas of members connecting the pairs of nodes 1-2, 1-4, 4-7, 7-10 are 9.52×10^{-4}, 1.58×10^{-4}, 1.47×10^{-4}, 1.56×10^{-3} (m^2), respectively. Other stiff members indicated by thick lines have the upper-bound cross-sectional areas. Since nodes 4, 5, and 6 are unstable, we remove these nodes and replace the two members connected to the unstable nodes with one member.

Figure 5(b) shows final topology, which has almost the same deformation properties as the model shown in Figure 5(a). Note that the thin member connecting nodes 1 and 7 can be manufactured as a spring. When the upper bound of A_i is increased to 4.0×10^{-3} m^2, a different optimal topology with $R(\mathbf{A})$ = 0.580 is obtained as shown in Figure 6. Therefore, various topologies can be obtained, if necessary, by adjusting the parameters for constraints. Although the value of $R(\mathbf{A})$ decreases, a simpler topology can be obtained by intuition from the solution in Figure 5(b). By replacing a stiff triangle part with a single member, and changing support conditions, we can obtain a simplified topology with $R(\mathbf{A})$ = 0.397 as shown in Figure 7.

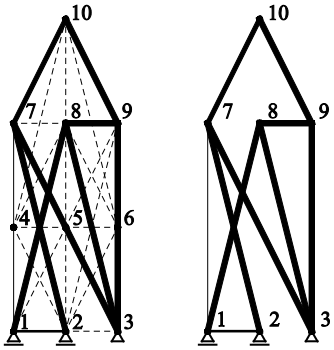

(a) (b)

Figure 5 Topology of the optimal solution

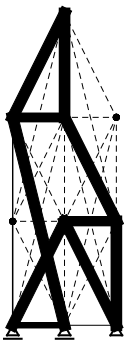

Figure 6 Optimal solution with A_i^U = 4.0×10^{-3} m^2

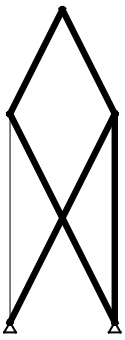

Figure 7 A simplified topology

4 Seismic response evaluation method and design response spectrum

We use the flexible supporting structure obtained in the previous section as a supporting structure of an arch, and carry out further optimization to reduce the roof response under horizontal seismic excitations. The maximum responses are evaluated using the complete quadratic combination (CQC) method [25] to

incorporate the correlation between the modes.

Let β_s and ϕ_s^j denote the sth participation factor and the jth component of the sth mode, respectively. The design acceleration response spectrum $S_a(T_s, h_s)$ is defined in terms of the natural period T_s and the damping factor h_s of the sth mode. For evaluation of acceleration response, the modal cross-correlation coefficient ρ_{sr} between the sth and rth modes is evaluated by [26]

$$\rho_{sr} = \frac{8\sqrt{h_s h_r}\left[h_r + \chi^3 h_s + 4\chi h_s h_r (h_r + \chi h_s)\right]\sqrt{\chi}}{\sqrt{(1+4h_s^2)(1+4h_r^2)\left[(1-\chi^2)^2 + 4h_s h_r \chi(1+\chi^2) + 4(h_s^2+h_r^2)\chi^2\right]}}, \quad (5)$$

$$\chi = \frac{\omega_r}{\omega_s}, \quad (6)$$

where ω_s and ω_r are the sth and rth natural circular frequencies, respectively. Then, the maximum absolute acceleration $\ddot{u}_j$ of the jth displacement component is evaluated by

$$\ddot{u}_j = \sqrt{\sum_{s=1}^{N}\sum_{r=1}^{N}(\beta_s \phi_s^j S_a(T_s, h_s))\rho_{sr}(\beta_r \phi_r^j S_a(T_r, h_r))}\ . \quad (7)$$

The number of modes N is 14 in the following examples. The following design acceleration response spectrum for a middle level earthquake with second rank soil condition specified in Japanese design code is used:

$$S_a(T_s, h_s) = \frac{1.5}{1+10h_s}\begin{cases} 0.96 + 9.0T_s & \text{for } T_s \le 0.16 \\ 2.4 & \text{for } 0.16 \le T_s \le 0.864 \\ 2.074/T_s & \text{for } 0.864 \le T_s \end{cases} \quad (8)$$

The design acceleration spectrum with damping factor h = 0.05 is shown in a thick line in Figure 8. For the time-history analysis in Section 5, ten seismic ground motions are generated to be compatible with the design response spectrum using random phase. The acceleration response spectra of ten ground motions are shown in thin gray lines in Figure 8. The time increment and the duration of each ground motion are 0.01 s and 60 s, respectively. The time history of one of the ground accelerations is shown in Figure 9.

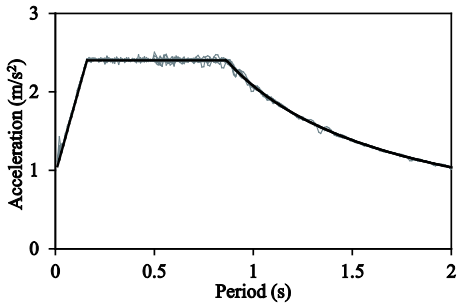

Figure 8 Acceleration response spectra (h=0.05); thick line: design spectrum, thin lines: spectra of ten ground motions

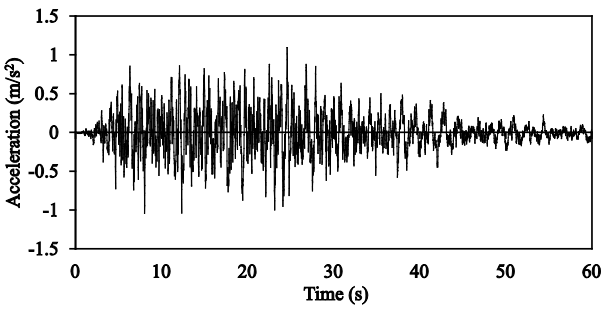

Figure 9 Time history of a ground acceleration

5 Flexible supporting structure of an arch

5.1 Arch with stiff supporting structure

In this section, we first summarize the vibration properties of an arch with conventional stiff supporting structures as illustrated in Figure 10. The span between the two top nodes of the supporting structures is 19.5 m and the height at the center of the roof is 8.61 m. The roof structure consists of ten steel beam members with Young's modulus 2.05×10^5 N/mm^2. The cross-sectional area and second moment of area of the beam are 4.68×10^{-3} m^2 and 7.21×10^{-5} m^4, respectively. The cross-sectional area of the steel tie bar that connects nodes 10 and 20 is 1.0×10^{-3} m^2, and that of the truss members of the supporting structure is 2.0×10^{-3} m^2. The mass of 800 kg is attached at nodes 10 to 20 to represent the mass of the roof structure. The mass of 400 kg is assign to the nodes in the supporting structure except supports; thus, the total mass of the arch and supporting structure is 13600 kg. We call this arch *stiff-model*.

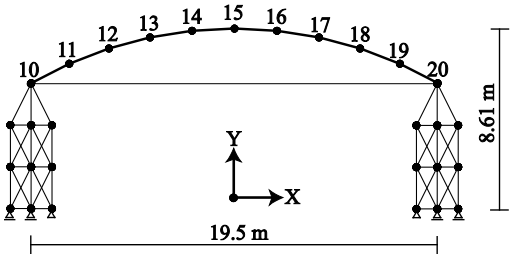

Figure 10 An arch with stiff supporting structures (stiff-model); thickness of each member is proportional to its cross-sectional area.

The properties of four lowest modes of the stiff-model are listed in Table 1, and the mode shapes are shown in Figure 11. The effective mass ratio of the *s*th mode in the *k*-directional component $\overline{M}_s^k$ $(k\in\{\mathrm{X},\mathrm{Y}\})$ shown in Table 1 is calculated by

$$\overline{M}_s^k=\frac{\left(\beta_s^k\right)^2}{M^k}, \tag{9}$$

where β_s^k and M^k are the *s*th participation factor in the *k*-directional component and the total mass in the *k*-directional component, respectively. The damping factor of each mode is defined as Rayleigh damping, where the damping factors of the 1st and 2nd modes are 0.02. It is noticed from Figure 11 that deformation of the roof structure is much larger than that of the supporting structures.

Table 1 Modal properties of the stiff-model

Mode	Period T_s [s]	Damping factor h_s	Effective mass ratio in X-dir $\overline{M}_s^{\mathrm{X}}$ [%]	Effective mass ratio in Y-dir $\overline{M}_s^{\mathrm{Y}}$ [%]
1st	0.369	0.0200	14.15	0.00
2nd	0.194	0.0200	0.00	22.44
3rd	0.135	0.0236	0.00	27.30
4th	0.124	0.0249	68.44	0.00

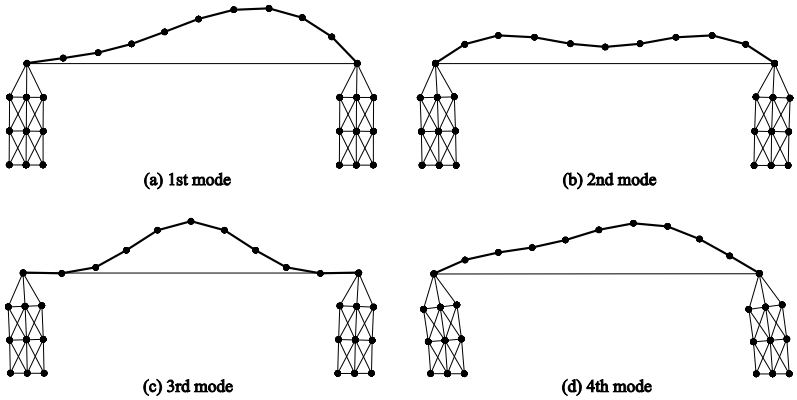

Figure 11 Four lowest modes of the stiff-model

5.2 Optimization of arch with flexible supporting structure

The flexible supporting structure obtained by topology optimization in Section 3 is attached at both ends of the arch as shown in Figure 12. The supporting structures are located symmetrically to make the roof displace in the tangential direction as illustrated in Figure 2. The mass of each node in the supporting structures except its supports is 800 kg so that this arch model has the same total mass as the stiff-model.

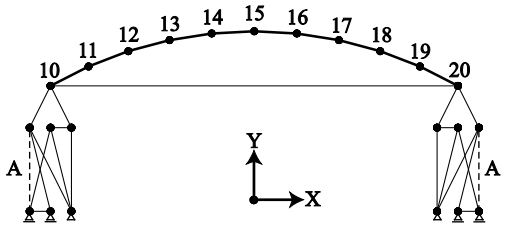

Figure 12 An arch model with flexible supporting structures

Through preliminary time-history seismic response analysis, it has been found that the stiffness of member A indicated by dashed lines in Figure 12 has a significant effect on the acceleration response of the roof structure. Therefore, the cross-sectional area of member A is chosen as a single design variable in the following optimization problem. The cross-sectional areas of the other members of supporting

structures are fixed at 2.0×10^{-3} m^2. The objective function to be minimized is evaluated by

$$F(A_{\mathrm{A}})=\sqrt{\frac{1}{9}\sum_{i=11}^{19}\left(\ddot{u}_i^n(A_{\mathrm{A}})\right)^2}\ , \tag{10}$$

where $\ddot{u}_i^n$ is the absolute acceleration response in the normal direction of the *i*th node evaluated by the CQC method, and A_{A} is the cross-sectional area of member A. The number of modes *N* in Eq. (7), used for the CQC method, is 14 so that the sum of the effective mass ratio in X-direction exceeds 95 %.

Let d_{gh} and d_{gv} denote X- and Y-directional displacements of the top node of the left supporting structure under self-weight. Lower bounds $d_{gh}^L = -0.012$ m and $d_{gv}^L = -0.0072$ m are assigned so that the supporting structure has enough vertical stiffness. Note that the lower bound d_{gv}^L is relaxed to 120 % of that of Problem 1 in Section 3 to have sufficiently large feasible region. The lower and upper bounds A_{A}^L and A_{A}^U for A_{A} are the same as those for A_i in Section 3. Hence, the optimization problem is formulated as:

$$\begin{aligned}\text{Problem 3:}\quad &\text{Minimize} && F(A_{\mathrm{A}})\\ &\text{subject to} && d_{gh}(A_{\mathrm{A}})\ge d_{gh}^L,\\ & && d_{gv}(A_{\mathrm{A}})\ge d_{gv}^L,\\ & && A_{\mathrm{A}}^L\le A_i\le A_{\mathrm{A}}^U,\end{aligned} \tag{11}$$

5.3 Optimization results

The cross-sectional area A_{A} is optimized to find the optimal value 8.765×10^{-5} m^2. The optimal objective value is 3.08 m/s^2, which is 57 % of that of the stiff-model. This solution is called *flexible-model*. Table 2 and Figure 13 show the modal properties and mode shapes, respectively, of the flexible-model. As seen from Table 2, the 1st natural period of the flexible-model is 1.2 times as large as that of the stiff-model. As shown in Figure 13, the large deformation is produced in the supporting structure in all modes, and the 1st mode exhibits the similar deformation property as illustrated in Figure 2.

Table 2 Modal properties of the flexible-model

Mode	Period T_s [s]	Damping factor h_s	Effective mass ratio in X-dir $\overline{M}_s^{\mathrm{X}}$ [%]	Effective mass ratio in Y-dir $\overline{M}_s^{\mathrm{Y}}$ [%]
1	0.4488	0.0200	49.194	0.000
2	0.3593	0.0200	1.235	0.000
3	0.2878	0.0210	0.000	50.771
4	0.1637	0.0284	0.000	2.395

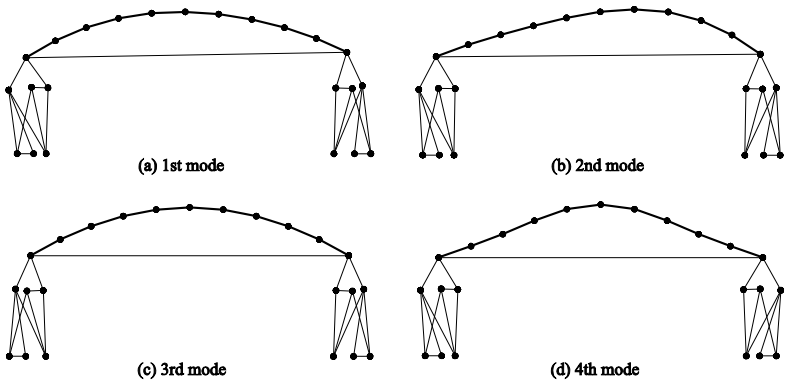

Figure 13 Four lowest modes of the flexible-model

5.4 Time-history response

Time-history analyses are carried out using the software OpenSees to obtain the maximum responses under ten ground motions. Note that the static analysis under self-weight is conducted before the time-history analysis. The mean values of the maximum absolute accelerations and the maximum displacements in the tangential and the normal directions of the nodes are plotted in Figure 14. The nodes are identified by X-coordinates. The maximum normal acceleration response among all the nodes of the flexible-model is 57 % of that of the stiff-model; on the other hand, the maximum tangential acceleration of the flexible-model increases to about 150 % of that of the stiff-model, because the support is optimized to enhance tangential displacement of the roof.

Figures 15(a)- 15(c) show the maximum values of the axial force, shear force, and bending moment of the roof members that exclude the cross-sectional forces under self-weight. Figures 15(d)- 15(f) show the maximum cross-sectional forces under only self-weight. It is noticed that the flexibility of the supporting structure reduces both the maximum shear force and bending moment, whereas increases them under self-weight. The effect of self-weight is not small in this case; however, it relatively diminishes with increase of the intensity of ground motions.

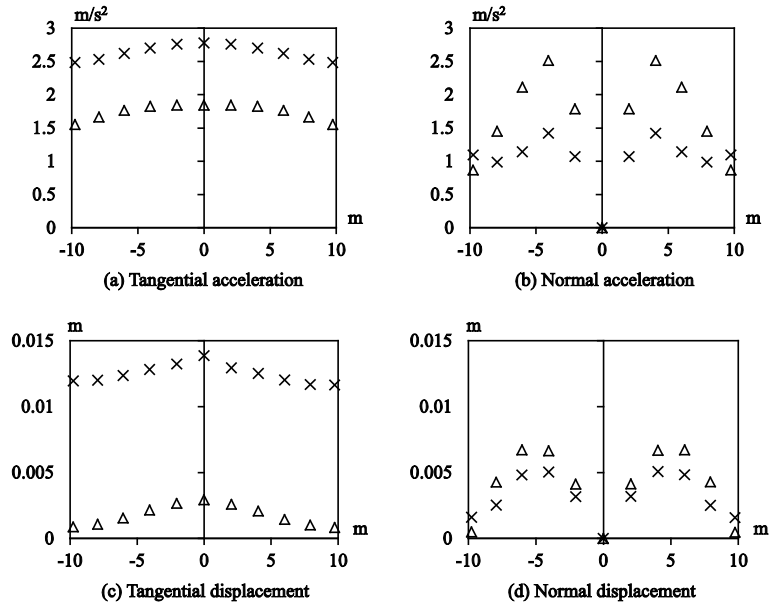

Figure 14 Mean-maximum responses of the acceleration and displacement; △: Stiff-model, ×:Flexible-model

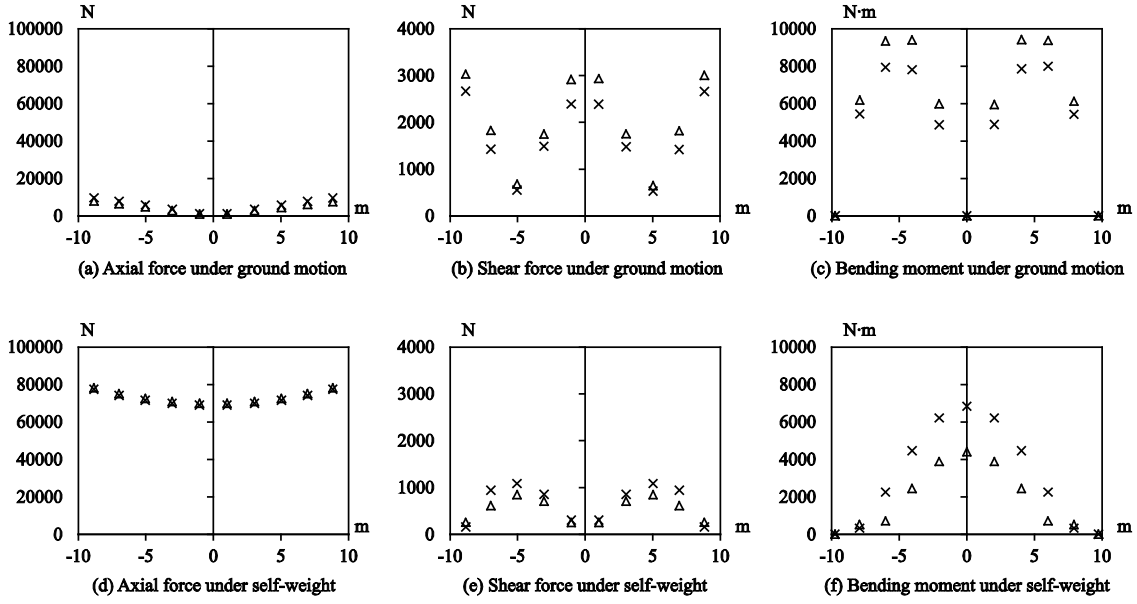

Figure 15 Mean-maximum cross-sectional forces of roof members; △: Stiff-model, ×:Flexible-model

5.5 Installation of passive energy dissipation device

In this section, we demonstrate the effectiveness of installing passive energy dissipation devices to the supporting structures in terms of reduction of the tangential response. As illustrated in Figure 16, viscous dampers are installed between the pairs of nodes 7, 8, and 7', 8', which have large relative displacements.

The relation between the damping coefficient of the dampers and the acceleration responses are shown in Figure 17. The vertical axis is the norm of acceleration response, defined in Eq. (10), obtained by time-history analysis under the ground motion described in Figure 9. As seen in Figure 17, the tangential acceleration decreases substantially with the increase of the damping coefficient, whereas the normal acceleration increases slightly. The tangential acceleration is reduced by about 40 % without increasing the normal acceleration, when the damping coefficient is 5000 N·s/m.

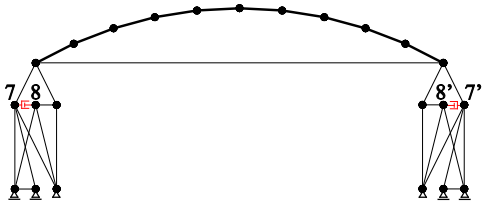

Figure 16 Location of the dampers

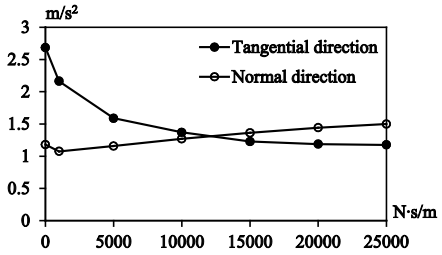

Figure 17 Relation between the damping coefficient and the acceleration response

Figure 18 shows the mean-maximum responses obtained by time-history analyses under ten ground motions. The results of the arch with/without dampers of 5000 N·s/m are plotted with ○ and ×, respectively. Installation of the dampers reduces the tangential acceleration at node 15 from 2.77 m/s^2 to 1.77 m/s^2, which is almost the same as that of the stiff-model plotted with △. The maximum cross-sectional forces without self-weight of the roof members are plotted in Figure 19, which indicates that the maximum shear force and the maximum bending moment are reduced to 80% and 81 %, respectively, by installing the dampers.

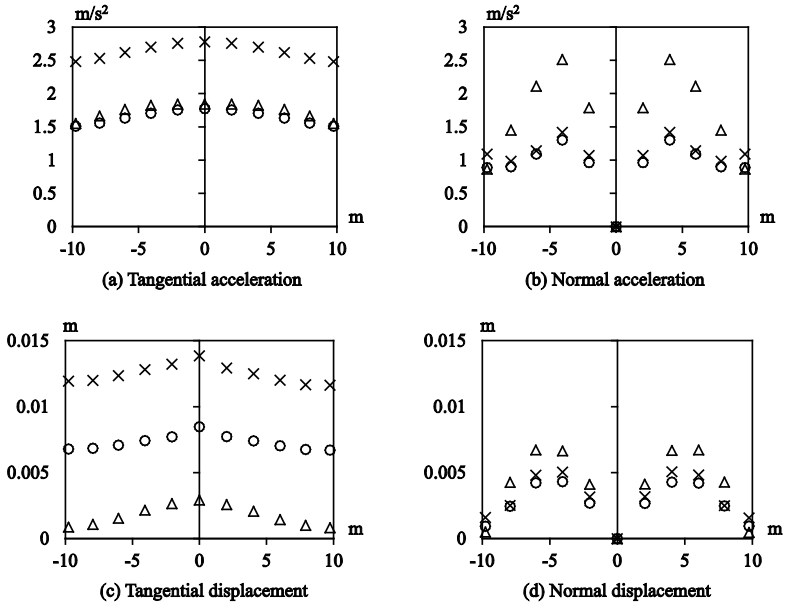

Figure 18 Mean-maximum acceleration and displacement responses; ○: Flexible-model with dampers, ×: Flexible-model without dampers, △:Stiff-model

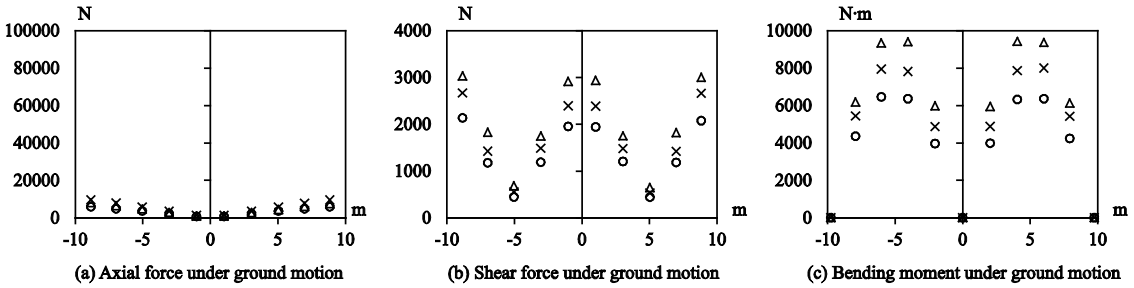

Figure 19 Mean-maximum cross-sectional forces of roof members; ○: Flexible-model with dampers, ×: Flexible model without dampers, △:Stiff-model

Figure 20(a) shows the time history of the normal acceleration response for five seconds at node 13, which has the largest mean-maximum value among all nodes. The dashed line and the solid line indicate the results of the stiff-model and the flexible-model with dampers, respectively. It is noticed that the vibration period of both models are nearly the same; on the other hand, the vibration period in the tangential direction has a large difference between the two models as seen in Figure 20(b). This is because the normal directional vibration is mainly caused by bending deformation of the roof members and the tangential directional vibration is affected by the vibration of the supporting structures.

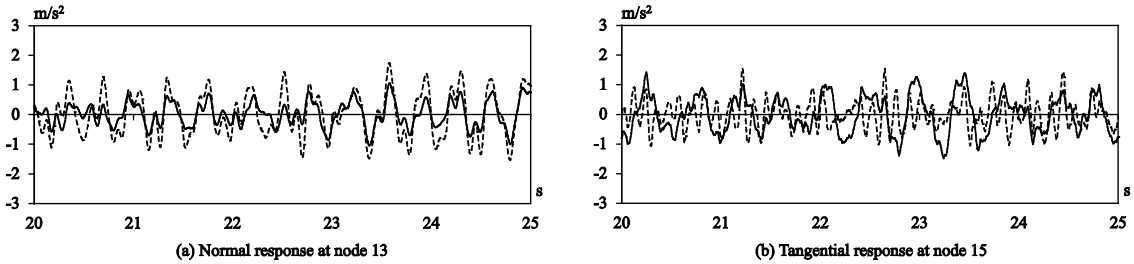

Figure 20 Time history of the acceleration response; dashed line: Stiff-model, solid line: Flexible-model with dampers

6 Conclusions

An optimization method has been presented for designing flexible supporting structures of an arch to reduce the acceleration response in the normal direction of the roof structure. The following conclusions have been obtained through this study:

1. The flexible supporting structure whose top node moves in the diagonal direction under a lateral load can be found by solving the optimization problem formulated as a nonlinear programming problem under static load. The ratio of the vertical displacement to the horizontal displacement is first maximized under constraints on stiffnesses in vertical and horizontal directions. The solution is further optimized to reduce the number of members by minimizing the total structural volume. Overestimation of structural volume using inverse power-law is effective to find an optimal truss with small number of members.
2. The acceleration response in the normal direction of the roof structure can be effectively reduced by adjusting the stiffness of the thin member in the flexible supporting structure. The responses are evaluated by the CQC method in optimization, and the response reduction by using the flexible supporting structure is confirmed by time-history analysis under spectrum-compatible ground motions.
3. Installing viscous dampers into the flexible supporting structure is very effective to reduce the tangential response without increasing the normal response. The proposed two-step approach can be used for controlling the direction of seismic response to reduce the displacement/acceleration in the specified direction.

Acknowledgement

This research is supported by JSPS KAKENHI Grant Number 26630257. The preliminary numerical analysis by Mr. Osamu Iwatsuki, former graduate student of Hiroshima University, is also appreciated.

Reference

1 Parulekar Y M, Reddy G R. Passive response control systems for seismic response reduction: A state-of-the-art review. Int J Struct Stab Dy, 2009, 9(1): 151–177

2 Pan P, Ye L P, Shi W, Cao H Y. Engineering practice of seismic isolation and energy dissipation in China, Sci China Tech Sci, 2012, 55(11): 3036–3046

3 Ohsaki M, Nakamura T, Isshiki Y. Shape-size optimization of plane trusses with designer's preference. J Struct Eng, 1998, 124(11): 1323–1330

4 Hoang N, Fujino Y, Warnitchai P. Optimal tuned mass damper for seismic application and practical design formulas. Eng Struct, 2008, 30(3): 707–715

5 Hasegawa T, Ohsaki M, Tsuda S. Parameter optimization of three-directional tuned mass damper for seismic response control. Korea: 8th China-Japan-Korea Joint Symposium on Optimization of Structural and Mechanical Systems (CJK-OSM8), 2014. Paper No. 0058

6 Tsuda S, Ohsaki M. Parameter optimization of mass damper consisting of compliant mechanism for bi-directional control of spatial structures (in Japanese). J Struct Constr Eng, 2012, 77(673): 379–387

7 Boroschek R, Moroni M O, Sarrazin M. Dynamic characteristics of a long span seismic isolated bridge. Eng Struct, 2003, 25(12): 1479–1490

8 Kinoshita T, Nakajima T, Ohsaki M. Topology optimization of compliant mechanisms for vertical seismic isolation of spatial structures. J Int Assoc for Shell and Spatial Struct, 2009, 50(2): 89–96

9 Wang H, Li A Q, Jiao C K, Spencer B F. Damper placement for seismic control of super-long-span suspension bridges based on the first-order optimization method, Sci China Tech Sci, 2010, 53: 2008–2014

10 Pan P, Ohsaki M, Kinoshita T. Constraint approach to performance-based design of steel moment-resisting frames. Eng Struct, 2007, 29: 186–194

11 Burns S (Ed.). Recent Advances in Optimal Structural Design: American Society of Civil Engineers (ASCE), 2002

12 Ohsaki M, Iwatsuki O, Watanabe H. Seismic response of building frames with flexible base optimized for reverse rocking response. Eng Struct, 2014, 74(1): 170–179

13 Wang Q, Lu Z Z, Tang Z C. A novel global optimization method of truss topology. Sci China Tech Sci, 2011, 54: 2723–2729

14 Ohsaki M. Optimization of Finite Dimensional Structures. Boca Raton, FL: CRC Press, 2010

15 Ohsaki M. Genetic algorithm for topology optimization of trusses. Comp Struct, 1995, 57(2): 219–225

16 Hajirasouliha I, Pilakoutas K, Moghaddam H. Topology optimization for the seismic design of truss-like structures. Comp Struct, 2011, 89: 702–711

17 Joint Editorial Committee for the Report on the Great East Japan Earthquake Disaster. Report on the Great East Japan Earthquake, Disaster Building Series Volume 3 (in Japanese). Tokyo: Maruzen

Publishing Co., 2014. 230–234

18 Bendsøe M P, Sigmund M. Topology Optimization: Theory, Method and Application. Berlin: Springer, 2003

19 Ohsaki M, Nakajima T, Fujiwara J, Takeda F. Configuration optimization of clamping members of frame-supported membrane structures. Eng Struct, 2011, 33: 3620–3627

20 Bruns T E. A reevaluation of the SIMP method with filterling and an alternative formulation for solid-void topology optimization. Struct Multidisc Optim, 2007, 30: 428–435

21 Guedes J M, Taylor J E. On the prediction of material properties and topology for optimal continuum structures. Struct Opt, 1997, 14: 193–199

22 Riez A. Sufficiency of a finite exponent in SIMP (power law) methods. Struct Opt, 2001, 21: 159–163

23 Gill P E, Murray W, Saunders M A. SNOPT: an SQP algorithm for large-scale constrained optimization. SIAM J Opt, 2002, 12: 97–1006

24 Open System for Earthquake Engineering Simulation (OpenSees). Pacific Earthquake Engineering Research Center, University of California, Berkeley. 2000

25 Wilson E L, Der Kiureghian A, Bayo E P. A replacement for the SRSS method in seismic analysis. Earthequake Eng Struct Dyn, 1981, 9: 187–194

26 Ohami K. A simple approximation formula of modal correlation coefficient in CQC method and its application examples (in Japanese). J Struct Constr Eng, 1999, 515: 83–89